The class II MHC protein HLA-DR1 in complex with an endogenous peptide: implications for the structural basis of the specificity of peptide binding

Venkatesh L Murthy[1] and Lawrence J Stern[2]*

Background: Class II major histocompatibility complex (MHC) proteins are cell surface glycoproteins that bind peptides and present them to T cells as part of the mechanism for detecting and responding to foreign material in the body. The peptide-binding activity exhibits allele-specific preferences for particular sidechains at some positions, although the structural basis of these preferences is not understood in detail. We have determined the 2.45 Å crystal structure of the human class II MHC protein HLA-DR1 in complex with the tight binding endogenous peptide A2(103–117) in order to discover peptide–MHC interactions that are important in determining the binding motif and to investigate conformational constraints on the bound peptide.

Results: The bound peptide adopts a polyproline II-like conformation and places several sidechains within pockets in the binding site. Bound water molecules mediate MHC–peptide contacts at several sites. A tryptophan residue from the β2 'lower' domain of HLA-DR1 was found to project into a pocket underneath the peptide-binding domain and may be important in modulating interdomain interactions in MHC proteins.

Conclusions: The peptide-binding motif of HLA-DR1 includes an aromatic residue at position +1, an arginine residue at position +2, and a small residue at position +6 (where the numbering refers to the normal MHC class II convention); these preferences can be understood in light of interactions observed in the peptide–MHC complex. Comparison of the structure with that of another MHC–peptide complex shows that completely different peptide sequences bind in essentially the same conformation and are accommodated with only minimal rearrangement of HLA-DR1 residues. Small conformational differences that are observed appear to be important in interactions with other proteins.

Addresses: [1]Johns Hopkins University School of Medicine, Baltimore, MD 21210, USA and [2]Department of Chemistry, Massachusetts Institute of Technology, Cambridge, MA 02139, USA.

*Corresponding author.
E-mail: stern@mit.edu

Introduction

Class II major histocompatibility complex (MHC) glycoproteins are found on the surface of B cells, macrophages, dendritic cells, and other specialized immune system cells. They bind peptides within endosomal compartments and present them at the cell surface for interaction with T-cell receptors as part of the immune system's mechanism for detecting and responding to foreign material in the body [1]. The interaction of peptide–MHC protein complexes with antigen receptors on the surface of T cells causes T-cell activation and stimulation of an immune response. In order to help stimulate immune responses against a wide variety of possible pathogens, MHC proteins can bind tightly to many different peptides. Class II MHC proteins isolated from B cells carry a wide spectrum of endogenous and exogenous peptides [2–4]. Analysis of these peptide mixtures and of the peptide-binding preferences of isolated class II MHC proteins has identified peptide-binding 'motifs', or patterns of preferred residues at

different peptide positions [5,6]. Peptide-binding motifs proposed for class II MHC proteins generally include residue preferences at positions 1, 4, 6 and 9, where position 1 is at an arbitrary point near the peptide N terminus, and where the particular residues preferred at these positions vary for different MHC allelic variants [7].

Structural characterization of class II MHC proteins bound to mixtures of endogenous peptides [8,9], or to single, defined peptides [10–12], has identified a general mode of peptide binding. Subsites or 'pockets' within the peptide-binding groove accommodate some of the bound peptide's sidechains. The residues lining the pockets appear to be responsible for the different motifs, or peptide-binding preferences of different allelic variants. The peptide termini do not play a major role in the binding mechanism, and can extend out from the site. This mechanism contrasts with that observed for class I MHC proteins, where peptides of sharply defined length bind through interactions

between the peptide termini and pockets at the ends of the peptide-binding site [13,14]. Although the basic mode of peptide interaction with class II MHC has been identified and subsites important to the peptide-binding specificity have been located, several important aspects of the peptide-binding interaction are not understood. These aspects include the extent of conformational variability allowed in the peptide-binding site, the role of solvent molecules in the binding interaction, and the structural basis for the observed peptide-binding motif.

Here we describe the crystal structure of HLA-DR1, a human class II MHC protein, in complex with a 15-residue endogenous peptide, and use the structure to help clarify these issues. The peptide A2(103–117) derives from the class I MHC protein HLA-A2 and is the predominant endogenous peptide bound to HLA-DR1 isolated from a B lymphoid cell line [2], presumably reflecting the abundance of the HLA-A2 protein in the endosomal subcellular compartment where peptide binding occurs. The A2 peptide conforms to the peptide-binding motif identified for HLA-DR1, and places the sidechains of 'anchor' residues tryptophan, leucine, and glutamine into MHC pockets 1, 4 and 9, respectively, and a glycine residue into pocket 6. Interactions observed in the crystal structure at the 'minor' anchor positions 2, 3 and 7 help to explain features of the peptide-binding preferences observed for HLA-DR1. Several water molecules are observed to mediate interactions between MHC residues and the bound peptide. Comparison of the structure of the HLA-DR1–A2 peptide complex with that previously determined for the HLA-DR1 complex with HA(306–318) [10], a peptide of completely different sequence, allows us to explore the plasticity of the peptide-binding site and the extent of conformational variation in the presence of different ligands. We also describe interactions among the peptide-binding and the immunoglobulin (Ig)-like domains, and explore the implications of the observed peptide conformational variability for T-cell activation.

Results and discussion
Structure determination
The structure of the complex of HLA-DR1 with A2(103–117) peptide was determined using diffraction data collected with synchrotron radiation and a single crystal cooled to −175°C (see Materials and methods section for details of data collection and refinement). Initial phase estimates were obtained by molecular replacement using the 2.75 Å model of the HLA-DR1–HA(306–318) peptide complex [10] with all peptide atoms omitted as the search model. Unambiguous electron density was observed for the bound peptide (Figure 1a). The initial electron-density maps were improved by iterative averaging of the noncrystallographically-related domains, and by cycles of manual model building and automated refinement (Figure 1b). The asymmetric unit contains four αβ complexes, arranged

as two copies of essentially the same $(\alpha\beta)_2$ dimer observed in other HLA-DR1 crystal structures [8–11,15,16]. Root mean square (rms) deviations between pairs of noncrystallographically-related domains range from 0.13 to 0.15 Å (see Materials and methods section). In keeping with the class II convention, we will refer to the peptide sidechain that projects into the large hydrophobic pocket near the N terminus as position +1, so the A2(103–117) peptide corresponds to positions −4 to +11.

Conformation of the bound peptide
The A2 peptide is bound in the peptide-binding site of HLA-DR1 in an extended, polyproline type II-like conformation (Figure 2a) as observed for other class II MHC–peptide complexes [10–12]. Both peptide termini extend from the site and are partially disordered. The core region of the peptide (positions −2 to +10) is well ordered and makes many contacts with HLA-DR1 (Table 1). The interaction between HLA-DR1 and the bound peptide covers just over half of the peptide surface, and buries 1750 Å^2 of molecular surface area [17]. The bound peptide is contacted by 36 MHC residues, with mostly polar atoms contacting the peptide mainchain, and mostly hydrophobic atoms contacting the sidechains in the principal sidechain-binding pockets 1, 4 and 9. At Ser(−2) the peptide kinks sharply (Figures 2a,b), orienting N-terminal residues Gly(−3) and Val(−4) towards the DR1β chain and breaking the polyproline repeat. In other class II MHC-peptide structures [10–12], electron density N-terminal to position −2 is weak but consistent with peptides extending straight out of the peptide-binding site. In the A2 peptide the kinked residues have little contact with MHC atoms (Table 1), and the kinked orientation may be specific to this peptide as it appears to be due to a set of electrostatic interactions linking the Gly(−3) mainchain, Asp(−1) carboxylate, and Arg(+2) guandinium groups.

The bound A2 peptide makes many interactions with HLA-DR1 through its mainchain atoms, and forms 14 hydrogen bonds directly with HLA-DR1 atoms (Figure 2b; yellow). Similar patterns of hydrogen bonding have been observed in other class II MHC structures [8–12] and proposed to play a general role in the tight binding of peptides; in particular, the asparagine and glutamine bidentate hydrogen bonds help to determine the polyproline conformation [8]. In addition to the direct HLA-DR1–peptide hydrogen bonds, several buried water molecules mediate hydrogen-bonding interactions between HLA-DR1 and the bound A2 peptide (Figure 2b; pink). Four of these water molecules are found as part of an elaborate hydrogen-bonding network underneath the central portion of the peptide (see below). A similar network has been observed in the murine class II MHC protein I-E^k and proposed to play a role in the pH dependence of peptide binding [12]. Three additional water molecules form hydrogen bonds

Figure 1

Peptide electron density. Maps calculated with $|2F_o-F_c|$ coefficients and model phases, contoured at 1σ, with peptide atoms omitted from the model. A side view of the peptide-binding site is shown, with the peptide running horizontally in the center of the figure with the N terminus on the left. The final model is superimposed on the map, with bonds colored according to atom type. Water molecules above and below the peptide are shown as spheres. **(a)** Map calculated with initial molecular replacement model. **(b)** Map calculated with final model.
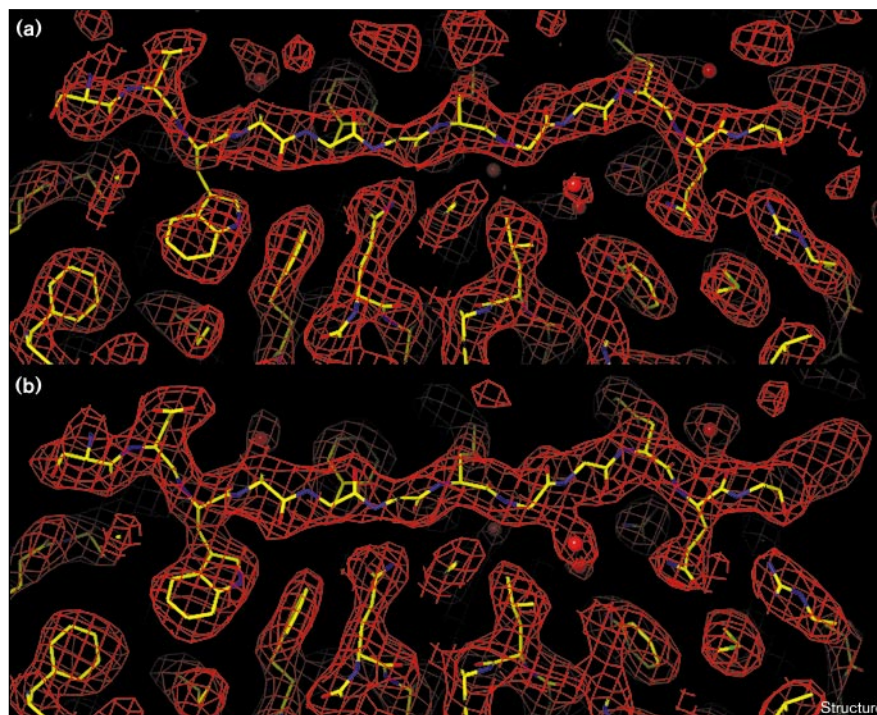
to exposed peptide mainchain atoms oriented away from the peptide-binding site (Figure 2b; blue).

Pockets in the peptide-binding site and the specificity of peptide binding

Interactions between sidechains from the bound peptide and pockets in the peptide-binding site are important in determining the peptide-binding affinity and sequence specificity of MHC proteins. The sidechains of the A2 peptide residues Trp(+1), Leu(+4) and Gln(+9) are buried in pockets in the binding site, with the sidechains of Arg(+2), Phe(+3) and Tyr(+7) also making substantial contacts in shallow pockets or 'shelves' within the overall peptide-binding site (Figure 2c; Table 1).

Pocket 1 is the largest [10] and most important [6,18,19] of the sidechain-binding pockets in HLA-DR1. The A2 peptide places tryptophan, one of the preferred 'anchor' residues at this position [6], into pocket 1. Unexpectedly, the tryptophan sidechain is oriented differently than the tyrosine found at this position in the HA peptide complex (Figure 3a). The new orientation corresponds to an approximately 80° rotation around the Cα–Cβ bond. In the new orientation, the tryptophan ring plane is perpendicular to Pheα24 (where α refers to the α subunit of HLA-DR1), with the indole nitrogen centered over the Pheα24 aromatic ring, apparently interacting with its π-electron cloud. Similar electrostatic interactions have been observed previously [20–22]. The sidechain rotation at position Trp(+1)

causes some alteration of the A2 peptide mainchain relative to that of the HA peptide, especially near the carbonyl of residue (–1) (Figure 3a). The different sidechains of the A2 and HA peptides, however, are accommodated with very little variation in the MHC residues that line pocket 1.

Pockets 4 and 9 of class II MHC proteins are also major pockets which bury substantial sidechain solvent-exposed surface area (Table 1). HLA-DR1 exhibits preferences for hydrophobic residues at these positions of the peptide, but hydrophilic residues with large aliphatic portions also are tolerated [6,18,23]. The A2 peptide places Leu(+4) into pocket 4, where it is ~90% buried by interactions with Pheβ13, Alaβ74 and Tyrβ78. The Gln(+9) sidechain of A2 peptide is oriented down into pocket 9, where it contacts a hydrophobic surface formed by atoms from Asnα69, Ileα72, Metα73, Trpβ9 and Trpβ61. The terminal amide of Gln(+9) packs against the salt bridge Argα76–Aspβ57 at the very bottom of the pocket. In both pockets 4 and 9 similar interactions were observed in the HLA-DR1–HA peptide complex [10].

Pocket 6 is also an important determinant of peptide binding, with HLA-DR1 preferring to bind peptides with small sidechains (glycine or alanine) at this position [6]. The A2 peptide has Gly(+6) at this position, and in the HLA-DR1–A2 peptide complex a water molecule binds in pocket 6 (Figure 3b). The water molecule can participate in hydrogen bonds with the A2 peptide mainchain nitrogen

Figure 2
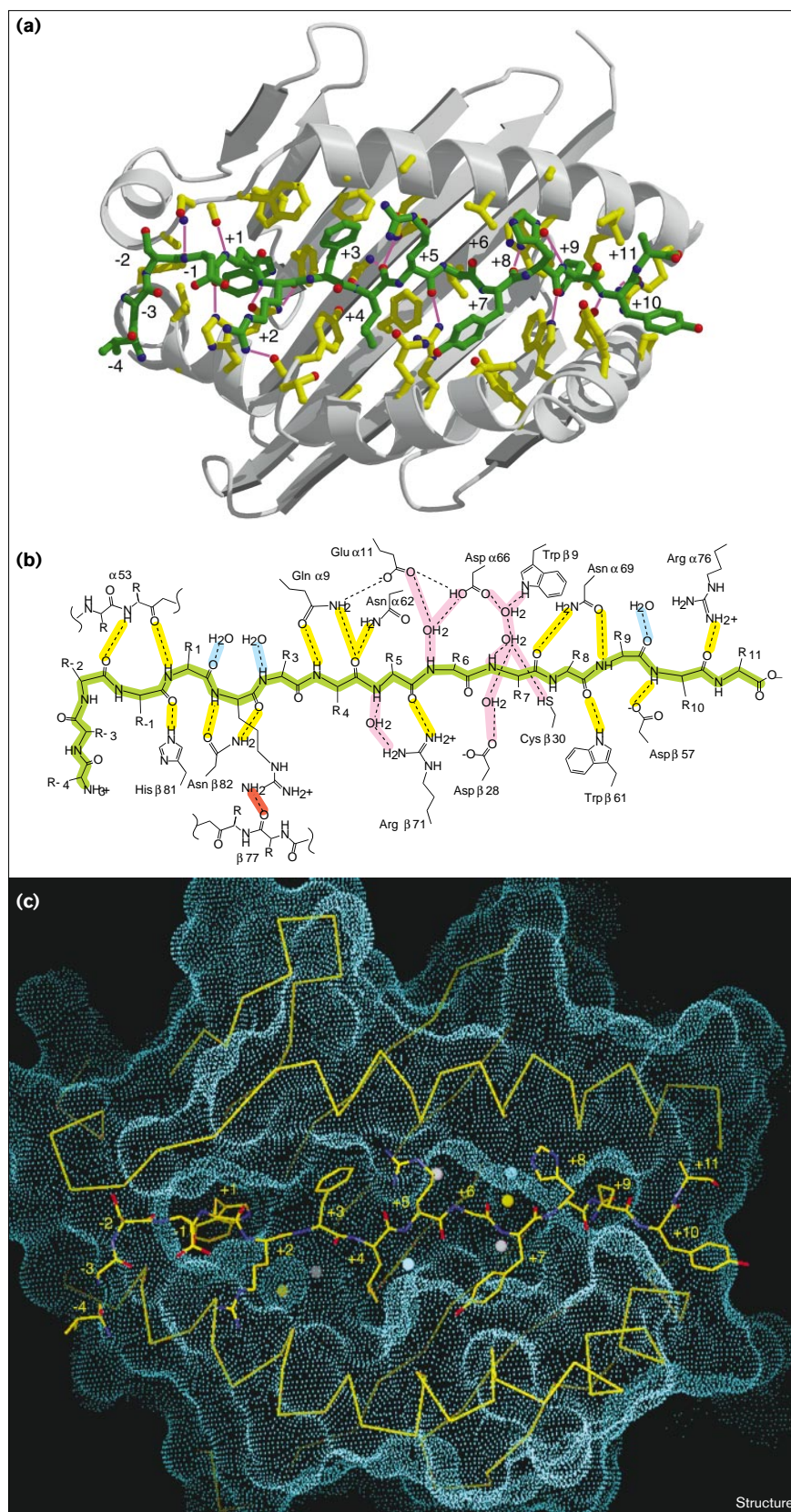
Structure of the HLA-DR1–A2 peptide binding site. **(a)** Top view of the peptide-binding site, with HLA-DR1 residues in contact with the peptide indicated with sidechain or mainchain atoms as appropriate. Atoms are colored by atom type, with oxygen in red, nitrogen in blue and carbon atoms in green for the peptide and yellow for HLA-DR1. The peptide residues are numbered, with Trp(+1) in the principal binding pocket; hydrogen bonds are shown in magenta. **(b)** Schematic diagram of peptide hydrogen-bonding interactions. The peptide sidechains are shown as R_n except for arginine at position 2 which contacts the HLA-DR1 mainchain carbonyl β77 at a kink in the β-chain helical region. The sidechain of His(+8) is also positioned to form a hydrogen bond with HLA-DR1 (not shown). The peptide mainchain is shaded in green. The interactions are color-coded: HLA-DR1–peptide hydrogen bonds, yellow; hydrogen bonds to buried water molecules, pink; hydrogen bonds to exposed water molecules, blue; Arg(+2) guanidinium–HLA-DR1 β77 carbonyl hydrogen bond, red. **(c)** Top view of the peptide-binding site, with the molecular surface indicated by blue dots. A Cα trace for HLA-DR1 is shown together with a stick model for the A2 peptide and buried water molecules; bonds are colored by atom type and water molecules are shown as spheres. Not all water molecules are observed in each molecule in the asymmetric unit.

Table 1

Peptide–MHC interactions.

Residue	Position	Buried area (Å^2)*	Mainchain contacts†	Sidechain contacts†
Val‡	−4	–	–	–
Gly	−3	14 (0.21)	(β81H) (β85V)	–
Ser	−2	62 (0.52)	α52 α53S β85V	α51 (α52 α53S)
Asp	−1	28 (0.35)	α53S β81 β85V	β81H
Trp	+1	230 (0.97)	α53 α54F β82N	α7I α24F α31I α32F α52A α53 β82N β85V β86
Arg	+2	95 (0.52)	α24F β78Y β82N	β77 β81H β82N
Phe	+3	93 (0.63)	α9Q β78Y	α9Q α22F α24F α54F α58 α62N
Leu	+4	154 (0.89)	α9Q α13Y α62N β78Y	β13F β74A β78Y
Arg	+5	94 (0.50)	α62N β13F β71R	α58 α61A α62N α65V
Gly	+6	54 (0.87)	α65V β11L	–
Tyr§	+7	160 (0.76)	α65V α69N β61W	β67L (β47Y β70Q β71R)§ (β60Y β61W β64Q)§
His	+8	73 (0.42)	α69N β60Y β68A α69N	α65V α68A α69N
Gln	+9	160 (0.96)	α69D α72I β61W β57D	α69N α72I α73M α76R β9W β57D β61W
Tyr	+10	106 (0.49)	α72I α76R β60Y β57D	α76R β56P β57D β60Y
Ala$^\#$	+11	0	–	–

*The solvent-accessible surface [55] in the free peptide that is sequestered upon formation of the MHC–peptide complex. Values are the average for four molecules in the asymmetric unit. The buried fraction (ratio of the buried area to the total solvent-accessible surface area for the residue in the free peptide) is shown in parentheses. Corresponding values for the molecular surface [17] follow the same trend and range from 0 Å^2 for Ala(+11) to 143 Å^2 (0.92) for Trp(+1). †MHC residues with atoms closer than 4 Å to peptide mainchain or sidechains are listed. Residues listed without amino acid names make contact through their mainchain only. Contacts that differ for the two orientations are indicated in parentheses. ‡Val(−4) is disordered and coordinates were not included in the model. Weak electron density at this position indicates minimal contact with HLA-DR1. §The sidechain of Tyr(+7) is found in two different orientations in different monomers in the asymmetric unit. $^\#$Ala(+11) makes no substantial contact with HLA-DR1.

at position (+6) and with HLA-DR1 residues Gluα11 and Aspα66 (Figure 2b). Alanine is another favored residue at this position and could bind in the pocket without displacing the bound water molecule by packing against Valα65 and Leuβ11. In the HA peptide, Thr(+6) binds into pocket 6 [10], shifting Asnα62, Valα65 and Aspα66 and displacing the bound water molecule (Figure 3b). Threonine is not a favored residue at position 6, and substitution of the HA peptide threonine by alanine increased binding affinity threefold [18]. This effect was also seen in a minimal, alanine-based peptide, where threonine to glycine substitution also caused an increase in peptide-binding affinity, ~tenfold [24]. Comparison of the HA and A2 peptide complexes in this region suggests that the threonine sidechain makes unfavorable polar–nonpolar contacts between its Cγ atom and polar residues near the water site, and between its sidechain hydroxyl group and Val α65. These changes are thought to be responsible for the decreased affinity.

The Arg(+2) sidechain of A2 peptide is not bound in a pocket (Figures 2b,c), but appears to play an important role in peptide binding to HLA-DR1. A preference for arginine at position (+2) was observed in studies of a minimal HLA-DR1-binding peptide, where the presence of arginine at this position provided an ~tenfold increase in binding affinity [23]. In the A2 peptide complex Arg(+2) is oriented up out of the binding site towards the β-chain helix, with one of its terminal nitrogen atoms hydrogen-bonding to the mainchain carbonyl oxygen of Thrβ77 (Figures 2a,b). Residue Thrβ77 is at a pronounced kink in the β-chain

helical region that accompanies a π helix→α helix transition (Figure 2a). The change in hydrogen-bonding pattern at the kink leaves the Thrβ77 carbonyl oxygen without an interhelical hydrogen bond. The interaction of the Thrβ77 carbonyl with the guanidinium of Arg(+2) appears to stabilize the helical structure by hydrogen-bonding with the free carbonyl oxygen. Interestingly, in the structure of the murine class II MHC protein I-E^k–Hb peptide complex, a threonine residue at position +2 plays a similar role by hydrogen bonding to the other lone pair of the free carbonyl oxygen at residue β77 [12].

In the structures of other class II MHC–peptide complexes [10,11], the peptide sidechains at positions 3 and 7 were observed to make substantial hydrophobic contacts with 'open pockets' or 'shelves' in the binding site. No strong sequence preferences are observed at these positions. The A2 peptide has Phe(+3) and Tyr(+7), both oriented upwards but making substantial hydrophobic contacts as they exit the peptide-binding site (Figure 2; Table 1). Phe(+3) is partly exposed in the complex which may mitigate any favorable interactions formed in the pocket. Tyr(+7) exhibits weak density and is found in two alternate conformations in different molecules in the asymmetric unit (Table 1). The β-chain helical region around pocket 7 is poorly determined and somewhat variable among class II MHC structures [8–12], and the variability around this pocket may be due to the influence of crystal contacts and intrinsic flexibility in this region of the protein.

Figure 3
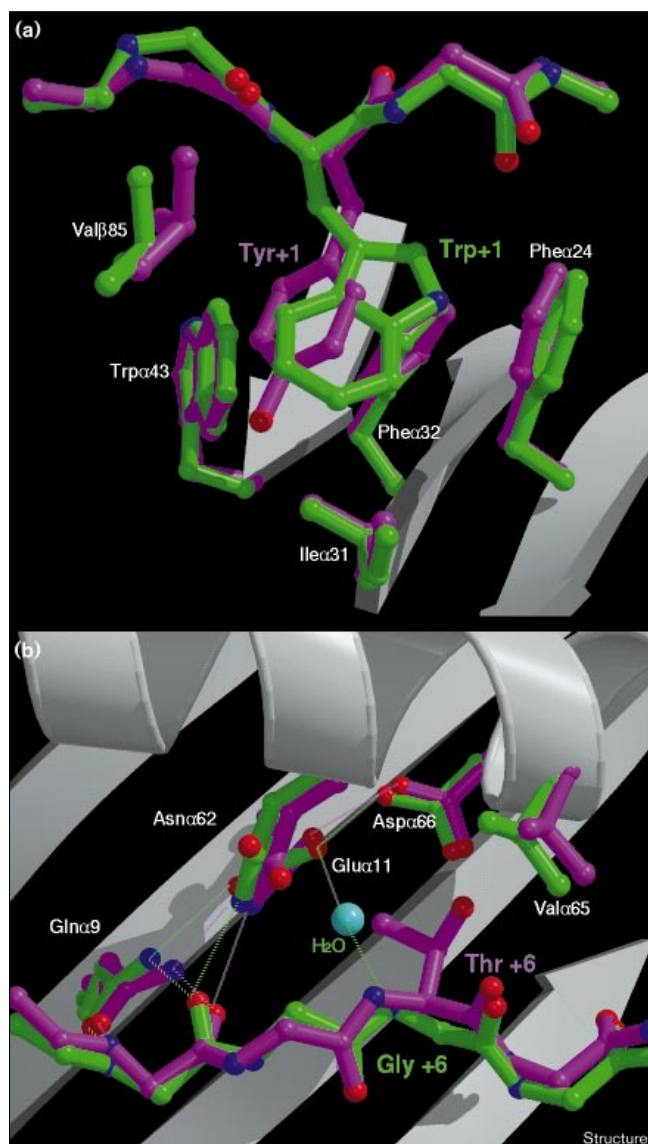
Pockets in the peptide-binding site. **(a)** Side view of pocket 1 in the A2 (green) and HA (purple) peptide complexes. The A2 peptide places a tryptophan sidechain into pocket 1, and the HA peptide places a tyrosine sidechain into this pocket. **(b)** Top view of pocket 4, colored as in (a). The A2 peptide has a glycine at position 4 and a water molecule (cyan) binds in the pocket in place of the sidechain; the HA peptide places a threonine sidechain into pocket 4 without bound water molecules. Hydrogen bonds are shown as dotted lines.

Buried water molecules

Three buried water molecules are found underneath the peptide in the region between pockets 6 and 7. One water molecule participates in hydrogen bonds with the A2 peptide amide nitrogen at position 7 and with Cysβ30 from the floor of the peptide-binding site (Figures 2b,c). This water molecule is also present in the HLA-DR1–HA peptide complex [10]. In many other class II alleles, tyrosine or histidine is found at position β30. These larger

sidechains can displace the water molecule, and directly form a hydrogen bond with the peptide amide nitrogen, as observed in the structures of the homologous human HLA-DR3 [11] and murine I-E[k] [12] class II MHC proteins. Binding sites for two other water molecules can be observed in this region, below the peptide between pockets 6 and 7 (Figures 2b,c). Water molecules in these sites can hydrogen bond with HLA-DR1 residues and with the water molecule described above bound to the peptide amide at position 7. This network of water molecules is variously occupied in the four molecules in the asymmetric unit, and has not been observed previously in lower resolution HLA-DR structures, although similar water molecules were observed in a murine I-E[k] peptide complex [12]. The buried water molecules may help to accommodate conformational variability between different peptides, and this region of the binding site exhibits the largest variability in peptide conformation among class II MHC peptide complexes determined to date [10–12]; the average mainchain deviation is ~1 Å for positions (+5) to (+8), compared with ~0.5 Å for positions (–1) to (+4). A similar role for bound water molecules in accommodating peptide conformational variability has been postulated in class I MHC proteins [25].

Potential sites for additional water molecules are also observed in the vicinity of pocket 1. In the structure of the HLA-DR1–HA peptide complex, two water molecules were observed in the bottom of pocket 1, apparently forming hydrogen bonds to Thrβ90 and the peptide's tyrosine hydroxyl group [10]. In the HLA-DR1–A2 peptide complex, the tryptophan sidechain of the bound peptide cannot provide a hydrogen bond to a water molecule bound to Thrβ90, and no ordered water molecules can be detected in this region. However, a void that could accommodate one to two water molecules is found adjacent to pocket 1 in all of the molecules in the asymmetric unit, and disordered solvent is likely to be present. Two water molecules occupy another site between pockets 1 and 4 in the HLA–DR1–A2 peptide complex (Figure 3c); these water molecules were not observed in the HLA-DR1–HA peptide complex. No naturally occurring peptide sidechain could displace any of the waters in this region without substantial peptide conformation rearrangement, and these additional water molecules may not be important for peptide sidechain selectivity.

Adjustment of the HLA-DR1 peptide-binding site to different peptides

Comparison of the structure of the HLA-DR1–A2 peptide complex with that observed for the HA peptide complex, shows that the peptides bind with similar conformation and in the same register (i.e. placing sidechains at positions 1, 4, 6 and 9 in pockets in the binding site; Figure 4a). The conformation of the HLA-DR1 protein mainchain is also essentially unchanged between the A2 and HA peptide complexes (Figure 4b). The largest mainchain deviations

Figure 4

Conformational flexibility in the peptide-binding site. **(a)** Side-view comparison of A2 (green) and HA (purple) peptides after alignment of the HLA-DR1 peptide-binding domains. **(b)** Comparison of MHC residues contacting the peptide for the A2 and HA complexes, top view, with residues contacting the A2 peptide in green and residues contacting the HA peptide in purple. Cα traces for the peptide-binding domains in the two complexes are shown. The positions of the sidechain-binding pockets (solid circles) and shelves (dotted circles) are shown. Light green triangles indicate the most significant alteration between HLA-DR1 bound to the HA or A2 peptide.
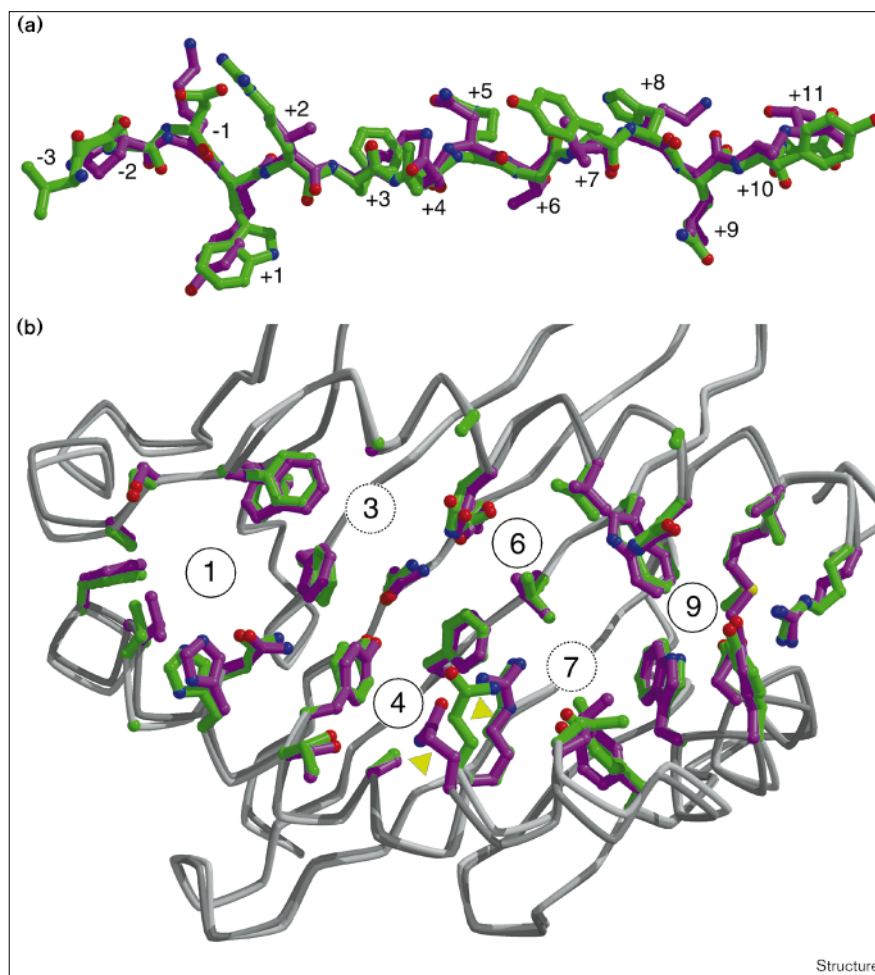

(~1.0–1.5 Å) occur at a kink in the β-chain helical region (β65–70) near pocket 7, a region that exhibits high B factors in all class II MHC structures and may be somewhat flexible. Smaller mainchain deviations (~1 Å) at the N-terminal end of the peptide-binding region (α50–51, β85–86) are consistent with slight rearrangements around pocket 1. Overall, the rms deviation between mainchain atoms in the binding domains of the A2 and HA peptide complexes is 0.45 Å, and standard deviations of corresponding phi and psi angles are 7° and 12°, respectively. All of these deviations are within the range observed between the four identical molecules in the HLA-DR1–A2 asymmetric unit. The pattern of hydrogen bonds between HLA-DR1 and the peptide mainchain atoms (Figure 2b) is also similar between the two complexes. There are only three differences in the hydrogen-bonding pattern within the A2 complex: the A2 peptide N-terminal kink prevents one hydrogen bond between the peptide (–2) amide nitrogen and HLA-DR1 residue α51; the Glnα9 terminal amide forms two hydrogen bonds with the peptide (+4) amide rather than one; and a bound water molecule substitutes

for one of the Asnα62 hydrogen bonds by interacting with the peptide amide nitrogen at position (+6).

Surprisingly, the different peptide sequences are accommodated with essentially no change in the conformation of the sidechains of MHC residues contacting the peptide (Figure 4b). The rms deviation for sidechains of residues that contact the peptide is 0.3 Å and the standard deviations of χ^1 and χ^2 angles for residues in contact with the peptide in the two structures are 8° and 10°, respectively. These values are essentially identical to the values for all residues in the peptide-binding domain (0.3 Å, 11° and 11°). Significant (> 1 Å) sidechain alteration between MHC residues in the A2 and HA peptide complexes is observed only at three places: β67, β70 and in pocket 1. The motion of Glnβ70 (Figure 4b; light green triangle) represents the largest change of MHC residues in the two structures. With Gln(+4) of the HA peptide bound in pocket 4, Glnβ70 at the end of the pocket forms hydrogen bonds with the exposed amide at the end of the sidechain. With A2 peptide Leu(+4) bound in pocket 4, Glnβ70 rotates

Figure 5
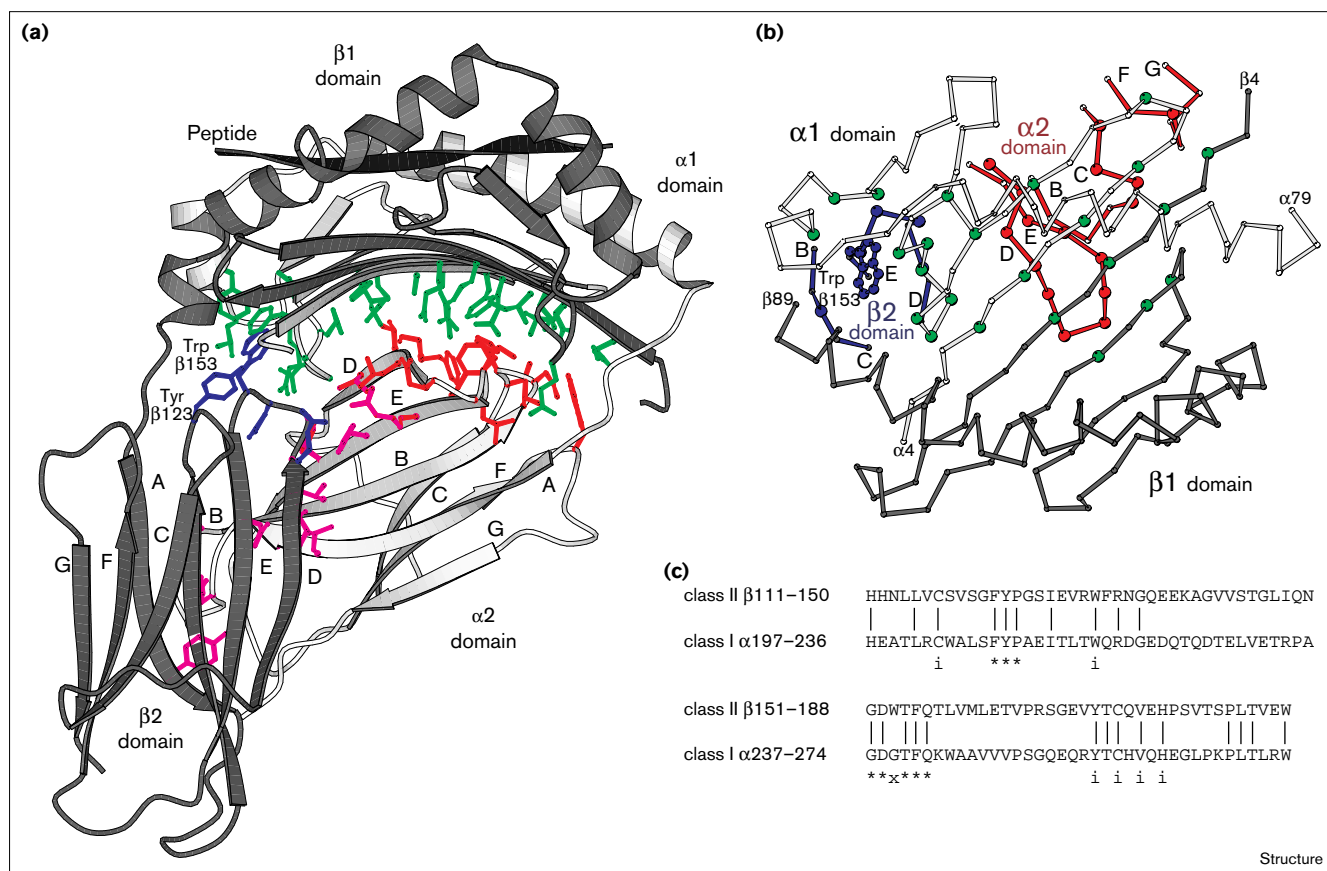
Domain interactions in class II MHC proteins. **(a)** Side view of the HLA-DR1 αβ heterodimer with the β subunit at the front and the peptide at the top. The protein is shown as a ribbon diagram with the α subunit in white, β subunit in gray, and the A2 peptide in dark gray; residues involved in domain interactions are indicated as colored sidechains or Cα atoms. Residues from the peptide-binding domain (α1β1) involved in interactions with the immunoglobulin-like domains α2 or β2 are colored green (α8, 10, 12, 14, 17, 21, 23, 26–31, 33, 44, 45, 48, β6, 8, 10, 12, 29, 31, 34); residues from α2 involved in interactions with the peptide-binding domain are colored red (α113–116, 135–146, 150, 168); residues from β2 involved in interactions with the peptide-binding domain are colored blue (β123, 149, 151–153); and residues involved in interactions between the α2 and β2 domains are colored magenta (α92–94, 96, 106, 135, 146, 148, 150, β102, 118, 120, 148–152, 156). **(b)** Top view of the peptide-binding domain. The α-chain helical region is shown at the top as a Cα trace with contact loops from the lower domains indicated. Cα atoms are only shown for contact residues, except for Trpβ153. Residue coloring is as in (a). **(c)** Sequences of class II β2 and corresponding class I α3 domains, with sequence identity (24% overall) indicated by vertical bars. Residues in contact with the peptide-binding domain are indicated by asterisks, and conserved immunoglobulin residues are indicated by the letter i. The position labeled x corresponds to tryptophan in all class II proteins and to glycine, or occasionally arginine, in class I proteins.

away from pocket 4 towards pocket 7, to make a hydrogen bond with the exposed hydroxyl group of Tyr(+7). Leuβ67 is located at the flexible kink of the β chain noted above, and shifts slightly between the A2 and HA peptide complexes to interact with the residue in pocket 7. Finally, several residues in pocket 1 show small reorientations in accommodating the A2 tryptophan anchor residue or the HA tyrosine anchor residue (Figures 3a and 4b). No other significant changes are observed between the two sites.

Interaction between domains

In addition to the peptide-binding domain described above, the class II MHC αβ heterodimer comprises two Ig-like domains, two transmembrane spans and two small cytoplasmic portions. Interactions between the different domains have not been described in detail as they have for class I MHC proteins [25,26]. These interactions are likely to be important in determining the patterns of MHC αβ chain pairing in heterozygotes, where several different α and/or β chains may be present [27–29], and may be important in orienting the molecule on the cell surface for interaction with receptors on other cells. We describe here the interactions between the extracellular α1β1 peptide-binding domain and the α2 and β2 Ig-like lower domains (Figure 5a). The peptide-binding domain contacts the lower Ig-like domains α2 and β2 at two sites. The larger contact site is formed by the underside of the β sheet from the peptide-binding domain (Figure 5; green) packing

against the edge and loops of the four-stranded β sheet from the α2 domain. This interaction buries 1200 Å^2 of molecular surface area, that would be accessible to solvent for the free domains, and consists of a hydrophobic patch formed by α2 residues from strand D and loops BC and DE (Figure 5; red), which contacts hydrophobic sidechains projecting from the underside of the peptide-binding site. Several residues surrounding this hydrophobic patch form reciprocal polar sidechain–mainchain interactions. The other contact area between the peptide-binding domain and Ig-like domains (750 Å^2) is formed by the BC and DE loops at the top of the β2 domain (Figure 5; blue), which project into a hydrophobic pocket underneath the left-hand side of the peptide-binding domain. This interaction is dominated by Trpβ153 which extends from the β2 DE loop to interact with several α1 and β1 residues underneath the left-hand side of the peptide-binding domain (Figure 5b), near pocket 1 (see below). Tyrβ123 from the BC loop also projects up to contact the peptide-binding domain. Finally, an additional interaction (450 Å^2) is formed between the two lower domains α2 and β2 (Figure 2a; magenta), which pack at an ~100° angle. This interaction comprises mostly polar residues sandwiched between the four-stranded β sheets of each domain.

The domain structure and interdomain interactions of class II MHC proteins are very similar to those of class I MHC proteins, but the class II β2 domain is oriented ~15° away from the peptide-binding site relative to the corresponding class I α3 domain [9]. The class II β2 and class I α3 loop regions that contact the peptide-binding domain are highly conserved, with the sequences Phe-Tyr-Pro (BC loop) and Gly-Asp-x-Thr-Phe-Gln (DE loop) invariant in all mouse and human class I and class II MHC proteins (Figure 2c). In class II sequences the residue 'x' is Trpβ153, which forms the principal β2 peptide-binding domain contact described above. In class I sequences the residue x is usually glycine. (In some sequences arginine is found at this position, but the arginine sidechain has been shown to project away from the upper domain [30].) The presence of tryptophan or glycine at the top of the class I α3 or class II β2 loops may be responsible for the different orientation of these domains in class I and class II MHC proteins. The orientation of these domains allows formation of the class II crystallographic dimer of dimers [9,13], aligns the peptide-binding site relative to the membrane for interaction with the T-cell receptor, and controls the accessibility of the binding sites for the T-cell co-receptor CD8 [31,32] and CD4 [33] molecules on the β2 domain CD loop (Figure 5a).

Biological implications
Class II major histocompatibility complex (MHC) molecules are type I transmembrane glycoproteins that bind a large variety of peptides in intracellular endosomal compartments and bring them to the cell surface for inspection by receptors on T cells. Along with the related class I MHC proteins, which generally bind peptides that are produced in the cytoplasm and transported to the endoplasmic reticulum, they provide T cells with a sample of peptides derived from the endogenous and exogenous proteins to which the cell has been exposed. Peptide selection by class II MHC proteins can be characterized by 'motifs' consisting of sidechain preferences at particular positions within the peptide. Motifs have been characterized for many allelic variants of class II MHC proteins [7], and the three structures that are available for complexes of class II MHC proteins with single peptides have generally shown significant MHC–peptide interaction at positions described in the corresponding motifs [10–12]. Despite these studies, however, the relationship of the observed binding preferences to the structure of the binding site is not yet understood in detail, particularly by comparison with the understanding of peptide binding by class I MHC proteins [13]. For example, it is not possible to predict the effect on the binding motif of MHC polymorphisms observed among human class II MHC proteins. This ability would be important in understanding the linkage between the MHC genotype and certain autoimmune diseases [34], and in predicting the antigenicity of potential therapeutic agents.

In an effort to understand the structural basis for the observed peptide specificity of HLA-DR1, a common human class II MHC protein, and to determine the extent of conformational variability allowed for bound peptides, we have determined the three-dimensional structure of HLA-DR1 in complex with a tight binding endogenous peptide A2(103–117). The structure reveals several peptide–MHC interactions that appear to be important in determining the binding motif. In addition, the relatively high resolution of the structure (2.45 Å) allowed us to locate several water molecules in subsites within the peptide-binding cleft. Variable binding of such water molecules would appear to facilitate the tight binding of different peptide sidechains in some of the peptide-binding pockets. Comparison of the structure of the HLA-DR1–A2 peptide complex with that previously determined for HLA-DR1 in complex with a different peptide [10] shows that completely different peptide sequences can adopt essentially the same bound conformation, with little or no adjustment of the MHC protein residues.

The HLA-DR1–A2 peptide structure provides insight into interactions of class II MHC proteins with other physiological effectors. T cell receptor proteins bind across the MHC peptide-binding site, contacting exposed regions of the bound peptide and the adjacent MHC α-helical regions [35]. Although the conformation of

peptides bound to HLA-DR1 [8] and other class II MHC proteins [11,12] is relatively stereotyped, the prediction of important T-cell receptor–peptide contacts at a physiologically significant level of detail may be difficult. For example, alteration of wholly buried residues is known to alter peptide recognition by particular T-cell clones [36–38]. The peptide mainchain rearrangement observed above one of the peptide-binding pockets, pocket 1, as HLA-DR1 accommodates tryptophan of the A2 peptide or tyrosine of the HA peptide appears to be such a case, as T-cell clones have been isolated that distinguish tyrosine from tryptophan at this position (in the context of another peptide bound to HLA-DR1) [39]. This rearrangement involves motions of only a few atoms over distances of less than 1 Å, and highlights the potential selectivity of the T-cell receptor–MHC interaction. Regions of the bound peptide outside the 'core' region could also influence T-cell receptor recognition if they fold back onto the MHC helical regions, as observed for the N terminus of the A2 peptide. A bent or kinked conformation for the bound peptide could explain the effect of C-terminal flanking tryptophan residues on T-cell recognition of a peptide bound to the murine MHC protein I-A^k [40]. It is possible that the bound peptide could also interfere with other proteins involved in T-cell recognition, as previously observed for the staphylococcal toxin responsible for toxic shock syndrome [15]. In the HLA-DR1–A2 peptide complex, two of the peptide residues (an aspartate and an arginine residue) partially block access to Hisβ81 and might be expected to interfere with binding of the 'superantigen' staphylococcal enterotoxin A (SEA), which is believed to bind to HLA-DR1 through coordination of Hisβ81 by a toxin-bond zinc ion [41–43]. Finally, interdomain motions mediated by residues at the domain interfaces may be important in orienting the peptide-binding site relative to the cell membrane for interaction with receptors on other cells.

Materials and methods
Production of the HLA-DR1–A2 peptide complex
HLA-DR1 was produced in baculovirus-infected Sf9 insect cells as soluble empty αβ heterodimers as described [44], except that both *DRA*0101* and *DRB1*0101* genes were carried on a single dual-promoter recombinant baculovirus. This system provided two- to fourfold increased HLA-DR1 expression levels and more consistent infection than the two-virus system. Regions corresponding to the entire extracellular domains were expressed (amino acid residues α1–192, β1–198). To construct the dual-promoter vector, the *Eco*RV-*Kpn*I fragment containing the polyhedrin promoter and *DRA*0101* gene was excised from pACDRA [44], the *Kpn*I 3′, overhang was filled in using Klenow fragment, and the resultant blunt-ended DNA was ligated into *Eco*RV-linearized pACDRB1 [44] to produce the final plasmid which carries two polyhedrin promoters in the same orientation. The dual-promoter plasmid was used to produce high-titer viral stocks by homologous recombination, as previously described. Soluble HLA-DR1 was isolated by immunoaffinity chromatography from serum-free medium used to grow baculovirus-infected Sf9 insect cells as described [44]. The peptide A2(103–117) VGSDWRFLRGYHQYA is a predominant self-peptide bound to HLA-DR1 isolated from a B lymphoid cell line, with longer and shorter versions of the same sequence observed at

lower abundance [2]. The A2 peptide was synthesized using 9-fluorenylmethyl carbonyl (FMOC) chemistry, purified by reverse-phase high pressure liquid chromatography (HPLC), and characterized by fast-atom bombardment (FAB) mass spectrometry to verify complete deprotection and lack of unexpected modifications. Purified HLA-DR1 was incubated with a fivefold molar excess of A2 peptide at 37°C, pH 7.0, and the resultant complex was purified by gel filtration.

Crystallization and data collection
Crystals of the HLA-DR1–A2 complex grew as needles from 10 mg/ml protein, 15% PEG 4000, 100 mM glycine, pH 3.5, at room temperature over approximately one week. A single crystal (40 μm × 40 μm × 300 μm) was transferred to 25% w/w glycerol in the crystallization solution by sequential incubation with increasing glycerol concentration over the course of 30 min. The crystal was mounted in a nylon fiber loop, rapidly cooled to −175°C and maintained at this temperature with a stream of cold N_2 gas. Diffraction data were collected using synchrotron radiation at the MacCHESS facility F1 beamline (λ = 0.908 Å) as a series of 1° oscillation photographs on storage phosphor image plates. Unit cell dimensions were a = 134.51, b = 134.32, c = 131.23, α = γ = 90°, β = 104.82°. Diffraction intensities were integrated and scaled using Denzo and Scalepack (W Minor and Z Otwinoski, unpublished data) (Table 2). The space group was found to be C2 by comparison of the intensity of reflections related by potential symmetry elements, with four HLA-DR1 αβ heterodimers per asymmetric unit. An overall isotropic B factor was estimated to be 37 Å from a Wilson plot, with no evidence of B-factor anisotropy. Data collection statistics are given in Table 2.

Molecular replacement
Initial phases were determined by molecular replacement using AMoRe [45], with a 2.75 Å structure of HLA-DR1 complexed with the HA peptide PKYVKQNTLKLAT [10] as search model. This model comprised the noncrystallographic $(\alpha\beta)_2$ dimer of heterodimers and included residues 5–180 of 192 residues in the α chain and residues 5–190 of 198 residues in the β chain. The peptide was omitted from the search model. Rotation search using 8 to 4 Å data and the $(\alpha\beta)_2$ dimer of heterodimers revealed four peaks of greater than 11.8σ (standard deviation above the mean rotation function) with no other peaks above 8.9σ, corresponding to two unique solutions each twofold degenerate about the $(\alpha\beta)_2$ dimer axis. The presence of $(\alpha\beta)_2$ dimers was confirmed by repeating the rotation search using a single αβ heterodimer, which resulted in four corresponding unique solutions of slightly weaker intensity (8.4–9.6σ). Similar results were obtained using other resolution limits. Translation search in the xz plane with one rotation search solution revealed a single peak of 17σ. This molecule was fixed and a three-dimensional search was performed using the other rotation search solution, providing a single 37σ peak. After rigid-body refinement treating each heterodimer as a rigid unit the R factor was 0.336 and correlation coefficient 0.664, for all data 8–4 Å. The two $(\alpha\beta)_2$ heterodimers in the asymmetric unit are related by an 89° rotation, similar to the crystallographic fourfold screw axis relating $(\alpha\beta)_2$ heterodimers in the $P4_32_12$ space group observed for the HLA-DR1–HA structure. The αβ heterodimers within each $(\alpha\beta)_2$ are related by an approximate twofold rotation axis, with slightly different transformations relating the α1/β1/peptide, α2, and β2 domains (176–180°), as has been observed for other DR crystal structures [9–11]. A rotation search with a dimer of heterodimers constructed using strict twofold symmetry gave a weaker solution, confirming the departure from strict twofold symmetry. Electron-density maps calculated omitting individual subunits revealed clear density for the omitted regions. An omit map showing the peptide region and calculated using the initial molecular replacement model is presented in Figure 1.

Noncrystallographic averaging, model building and refinement
Iterative real space fourfold noncrystallographic averaging was used to improve the molecular replacement phases and to extend them from 3.0 Å to 2.45 Å. Separate molecular envelopes were generated for the peptide-binding domain (α1β1) and for each of the immunoglobulin domains (α2 and β2) using MAMA [46] and manual inspection of omit maps. Fourfold averaging of electron density was performed using RAVE [47], with the improved phases used to calculate new maps until

Table 2

Data collection and refinement statistics*.

Resolution range (Å)*	Reflections[†]	hkl[‡]	Redundancy[§]	Completeness[#]	I/σI[¶]	R$_{sym}$[¥]	R$_{cryst}$[**]	R$_{free}$[††]
20.00–5.99	10 521	4696	2.2	0.84	36.8	0.041	–	–
5.99–4.18	25 077	10 760	2.3	0.97	35.8	0.046	0.174	0.243
4.18–3.53	24 738	10 756	2.3	0.98	28.2	0.066	0.190	0.270
3.53–3.16	24 286	10 716	2.3	0.97	21.4	0.076	0.216	0.275
3.16–2.90	22 360	10 395	2.2	0.95	15.4	0.119	0.250	0.300
2.90–2.72	20 304	9709	2.1	0.89	9.4	0.167	0.263	0.317
2.72–2.57	17 348	8806	2.0	0.81	6.4	0.252	0.297	0.341
2.57–2.45	13 661	7700	1.8	0.70	4.4	0.331	0.319	0.354
20.00–2.45	157 895	73 538	2.1	0.85	14.9	0.070	–	–
6.00–2.45	147 770	68 842	2.1	0.89	14.0	–	0.216	0.279

*Resolution range 20.00–2.45 Å was used for maps and phase calculations and resolution range 6.00–2.45 Å was used for refinements. The model includes 1445 amino acid residues and 152 solvent molecules for 12 019 total atoms included in the refinement. [†]Number of reflections measured (observations). [‡]Number of independent hkl's measured. [§]Data redundancy (number of hkl's/observations). [#]Data completeness (hkl's measured/total possible hkl's). [¶]Data intensity (mean reflection intensity/estimated error). [¥]R factor (Σ |I(hkl)− <I>| /ΣI) on intensity for symmetry-related reflections. [**]R factor (Σ|F$_{obs}$−F$_{calc}$| / ΣF$_{obs}$) on structure factors for reflections used in refinement (90% of total). [††]R factor on structure factors for reflections omitted from the refinement and used as a test set (10% of total).

convergence. A model for the bound peptide was built and the initial DR1 model was adjusted using averaged electron-density maps that were calculated by omitting coordinates for the region under consideration. The rebuilt model was refined using X-PLOR [48] with rigid body, simulated annealing, positional, and restrained B-factor refinement steps. At this point the R factor for the model was 0.294 for all reflections 6–2.45 Å with F > 2σ$_F$, and the free R factor, calculated using reflections not included in any refinement steps and comprising 10% of the total reflections, was 0.326. Eight cycles of rebuilding and refinement brought the R factor to 0.217 and the free R factor to 0.288. After cycle three the phase averaging was discontinued although noncrystallographic symmetry (NCS) restraints relating the four molecules in the asymmetric unit were continued for all refinement steps. Atoms involved in crystal contacts were not included in the NCS restraints. The NCS restraint weights were determined by examination of the free R factor, with optimum restraints relating the two (αβ)$_2$ units tighter than those relating the two αβ molecules within each (αβ)$_2$ dimer. Water molecules were added based on peaks in F$_{obs}$− F$_{calc}$ difference maps identified using the CCP4 suite of programs [49] and ARP [50], and on hydrogen-bonding distance and geometry criteria. Refinement steps performed using REFMAC [49] were included in cycles seven, eight and nine. The final model includes coordinates for DR1 residues α3–α181 (of 192 residues), β4–β190 (of 198 residues), peptide residues A2 104–117 (of 103–118), and 152 water molecules (Table 2). Weak electron density was observed for the expected three carbohydrate moieties of HLA-DR1 but did not permit determination of an atomic model. The loop regions β106–111 and β166–168 exhibited weak electron density and large B factors, particularly in molecule three, and were modeled without sidechain occupancy in molecules one, two and four and were not included at all in molecule three. Residue Glnβ64 was disordered in all molecules and was not included in the model. These regions were also observed to be disordered in other class II structures.

Analysis
Model geometry was examined using Procheck [51] and found to meet or exceed criteria determined for structures of similar resolution. Only one residue, Asnβ33, fell outside allowed regions of a Ramachandran plot. The φ angle of this residue is unusual, allowing a turn to be formed with hydrogen bonds between the β33 sidechain, β8 backbone amide, and α80 backbone carbonyl. Rms deviation from ideal geometry is 0.016 Å for bond lengths, 2.53° for bond angles, and 26.0° for dihedral angles. Average coordinate error was estimated to be 0.3 Å by Luzzati analysis [52] and 0.27 Å by SIGMAA analysis [53]. Rms deviations between pairs of noncrystallographically-related molecules is 0.9 Å (molecules

one–three or two–four) or 1.8 Å (molecules one–two or three–four), but is considerably smaller, 0.3–0.5 Å, if the α1/β1/peptide, α2, and β2 domains are considered separately. The latter values are commensurate with the expected coordinate error. Standard deviations of symmetry-related torsion angles φ, φ, χ^1 and χ^2 are 6–7°. Average B factors are 40 Å^2 (mainchain) and 41 Å^2 (sidechain) for the MHC protein, 42 Å^2 for solvent molecules, and 51 Å^2 (mainchain) and 54 Å^2 (sidechain) for the peptide. Average RS-fit [54] values were 0.82 (mainchain) and 0.78 (sidechain) for both the MHC protein and the peptide, and 0.69 for the solvent. B factors and RS-fit values were not significantly different among the four molecules in the asymmetric unit. The programs ACCESS [55], and MS [17] were used to analyze solvent accessibility and molecular surfaces, LSQMAN [56] and LSQKAB [57] to determine relationships among the NCS-related molecules, and MOLSCRIPT [58], RIBBONS [59], RASTER 3D [60], O [54], and GRASP [61] to display the structure. To evaluate the significance of differences observed between the HLA-DR1–A2 complex determined here and other class II MHC crystal structures, we considered the rms deviations between NCS-related atoms not involved in crystal contacts and the expected coordinate error, and used these values in considering differences with other structures.

Accession numbers
Coordinates and structure-factor amplitudes have been deposited in the Brookhaven Protein Data Bank with accession code 1AQD.

References
1. Germain, R.N. & Margulies, D.H. (1993). The biochemistry and cell biology of antigen processing and presentation. *Annu. Rev. Immunol.* **11**, 403–450.
2. Chicz, R.M., *et al.*, & Strominger, J.L. (1992). Predominant naturally processed peptides bound to HLA-DR1 are derived from MHC-related molecules and are heterogeneous in size. *Nature* **358**, 764–768.
3. Rudensky, A.Y., Preston-Hurlburt, P., Al-Ramadi, B.K., Rothbard, J. & Janeway, C.A.J. (1992). Truncation variants of peptides isolated from MHC class II molecules suggest sequence motifs. *Nature* **359**, 429–431.
4. Hunt, D.F., *et al.*, & Sette, A. (1992). Peptides presented to the immune system by the murine class II major histocompatibility complex molecule I-A^d. *Science* **256**, 1817–1820.

5. Sette, A., *et al.*, & Grey, H.M. (1989). Prediction of major histocompatibility complex binding regions of protein antigens by sequence pattern analysis. *Proc. Natl. Acad. Sci. USA* **86**, 3296–3300.

6. Hammer, J., Takacs, B. & Sinigaglia, F. (1992). Identification of a motif for HLA-DR1 binding peptides using M13 display libraries. *J. Exp. Med.* **176**, 1007–1013.

7. Rammensee, H.-G. (1995). Chemistry of peptides associated with MHC class I and class II molecules. *Curr. Opin. Immunol.* **7**, 85–96.

8. Jardetzky, T.S., *et al.*, & Wiley, D.C. (1996). Crystallographic analysis of endogenous peptides associated with HLA-DR1 suggests a common, polyproline II-like conformation for bound peptides. *Proc. Natl. Acad. Sci. USA* **93**, 734–728.

9. Brown, J.H., *et al.*, & Wiley, D.C. (1993). The three-dimensional structure of the human class II histocompatibility antigen HLA-DR1. *Nature* **364**, 33–39.

10. Stern, L.J., *et al.*, & Wiley, D.C. (1994). Crystal structure of the human class II MHC protein HLA-DR1 complexed with an influenza virus peptide. *Nature* **368**, 215–221.

11. Ghosh, P., Amaya, M., Mellins, E. & Wiley, D.C. (1995). The structure of an intermediate in class II MHC maturation: CLIP bound to HLA-DR3. *Nature* **378**, 457–462.

12. Fremont, D.H., Hendrickson, W.A., Marrack, P. & Kappler, J. (1996). Structures of an MHC class II molecule with covalently bound single peptides. *Science* **272**, 1001–1004.

13. Madden, D.R. (1995). The three-dimensional structure of peptide–MHC complexes. *Annu. Rev. Immunol.* **13**, 587–622.

14. Stern, L.J. & Wiley, D.C. (1994). Antigenic peptide binding by class I and class II histocompatibility proteins. *Structure* **15**, 245–251.

15. Kim, J., Urban, R.G., Strominger, J.L. & Wiley, D.C. (1994). Toxic shock syndrome toxin-1 complexed with a class II MHC protein HLA-DR1. *Science* **266**, 1870–1874.

16. Jardetzky, T.S., *et al.*, & Wiley, D.C. (1993). Three-dimensional structure of a human class II histocompatibility molecule complexed with superantigen. *Nature* **368**, 711–718.

17. Connolly, M.L. (1983). Analytical molecular surface calculation. *J. Appl. Cryst.* **16**, 548–558.

18. O'Sullivan, D., *et al.*, & Sette, A. (1991). On the interaction of promiscuous antigenic peptides with different alleles. *J. Immunol.* **147**, 2663–2669.

19. Jardetzky, T.S., Gorga, J.C., Busch, R., Rothbard, J., Strominger, J.L. & Wiley, D.C. (1990). Peptide binding to HLA-DR1: a peptide with most residues substituted to alanine retains MHC binding. *EMBO J.* **9**, 1797–1803.

20. Burley, S.K. & Petsko, G.A. (1986). Amino–aromatic interactions in proteins. *FEBS Lett.* **203**, 139–143.

21. Dougherty, D.A. (1996). Cation-π interactions in chemistry and biology: a new view of benzene, Phe, Tyr and Trp. *Science* **271**, 163–168.

22. Perutz, M.F. (1993). The role of aromatic rings as hydrogen-bond acceptors in molecular recognition. *Phil. Trans. Phys. Sci.* **345**, 1674–1779.

23. Hammer, J., *et al.*, & Nagy, Z. (1994). High-affinity binding of short peptides to major histocompatibility complex class II molecules by anchor combinations. *Proc. Natl. Acad. Sci. USA* **91**, 4456–4460.

24. Hammer, J., *et al.*, & Sinigaglia, F. (1993). Promiscuous and allele-specific anchors in HLA-DR-binding peptides. *Cell* **74**, 197–203.

25. Fremont, D.H., Matsumura, M., Stura, E.A., Peterson, P.A. & Wilson, I.A. (1992). Crystal structures of two viral peptides in complex with murine MHC class I H2-K^b. *Science* **257**, 919–927.

26. Saper, M.A., Bjorkman, P.J. & Wiley, D.C. (1991). Refined structure of the human histocompatibility antigen HLA-A2 at 2.6 Å resolution. *J. Mol. Biol.* **219**, 277–319.

27. Braunstein, N.S., Weber, D.A., Wang, X.-C., Long, E.O. & Karp, D. (1992). Sequences in both class II major histocompatibility complex α and β chains contribute to the binding of the superantigen toxic shock syndrome toxin 1. *J. Exp. Med.* **175**, 1301–1305.

28. Karp, D.R., Teletski, C.L., Jaraquemade, D., Maloy, W.L., Coligan, J.E. & Long, E.O. (1990). Structural requirements for pairing of α and β chains in HLA-DR and DP molecules. *J. Exp. Med* **171**, 615–628.

29. Kwok, W.W., Kovats, S., Thurtle, P. & Nepom, G.T. (1993). HLA-DQ allelic polymorphisms constrain patterns of class II heterodimer formation. *J. Immunol.* **150**, 2263–2272.

30. Madden, D.R., Gorga, J.C., Strominger, J.L. & Wiley, D.C. (1992). The three-dimensional structure of HLA-B27 at 2.1 Å resolution suggests a general mechanism for tight peptide binding to MHC. *Cell* **70**, 1035–1048.

31. Gao, G.F., *et al.*, & Jakobsen, B.K. (1997). Crystal structure of the complex between human CD8αα and HLA-A2. *Nature* **387**, 630–634.

32. Salter, R.D., *et al.*, & Parham, P. (1990). A binding site for the T-cell co-receptor CD8 on the α$_3$ domain of HLA-A2. *Nature* **345**, 41–46.

33. Konig, R., Huang, L.-Y. & Germain, R.N. (1992). MHC class II interaction with CD4 mediated by a region analogous to the MHC class I binding site for CD8. *Nature* **356**, 796–798.

34. Tiwari, J.L. & Terasaki, P.I. (1985). *HLA and Disease Associations*. Springer-Verlag, NY.

35. Garboczi, D.N., Ghosh, P., Utz, U., Fan, Q.R., Biddison, W.E. & Wiley, D.C. (1996). Structure of the complex between human T-cell receptor, viral peptide, and HLA-A2. *Nature* **384**, 134–141.

36. Newton-Nash, D.K. & Eckels, D.D. (1993). Differential effect of polymorphism at HLA-DR1 beta-chain positions 85 and 86 on binding and recognition of DR1-restricted antigenic peptides. *J. Immunol.* **150**, 1813–1821.

37. Boehncke, W.-H., *et al.*, & Germain, R.N. (1993). The importance of dominant negative effects of amino acid sidechain substitution in peptide–MHC molecule interactions and T cell recognition. *J. Immunol.* **150**, 331–341.

38. Ong, B., *et al.*, & Newson-Davis, J. (1991). Critical role for the Val/Gly^{86} HLA-DRβ dimorphism in autoantigen presentation to human T cells. *Proc. Natl. Acad. Sci. USA* **88**, 7343–7347.

39. Wu, S., Gorski, J., Eckels, D.D. & Newton-Nash, D.K. (1996). T cell recognition of MHC class II-associated peptides is independent of peptide affinity for MHC and sodium dodecylsulfate stability of the peptide/MHC complex. *J. Immunol.* **156**, 3815–3820.

40. Vignali, D.A.A. & Strominger, J.L. (1994). Amino acid residues that flank core peptide epitopes and the extracellular domains of CD4 modulate differential signaling through the T cell receptor. *J. Exp. Med.* **179**, 1945–1956.

41. Hudson, K.R., Tiedemann, R.E., Urban, R.G., Lowe, S.C., Strominger, J.L. & Fraser, J.D. (1995). Staphylococcal enterotoxin A has two cooperative binding sites on major histocompatibility complex class II. *J. Exp. Med.* **182**, 711–720.

42. Herman, A., Labrecque, N., Thibodeau, J., Marrack, P., Kappler, J.W. & Sekaly, R.P. (1991). Identification of the staphylococcal enterotoxin A superantigen binding site in the b1 domain of the human histocompatibility antigen HLA-DR. *Proc. Natl. Acad. Sci. USA* **88**, 9954–9958.

43. Karp, D.R. & Long, E.O. (1992). Identification of HLA-DR1 β chain residues critical for binding staphylococcal enterotoxin A and E. *J. Exp. Med.* **175**, 415–424.

44. Stern, L.J. & Wiley, D.C. (1992). The human class II MHC protein HLA-DR1 assembles as empty αβ heterodimers in the absence of antigenic peptide. *Cell* **68**, 465–477.

45. Navazza, J. (1994). AMoRE: an automated package for molecular replacement. *Acta Cryst. A* **50**, 157–163.

46. Kleywegt, G.J. & Jones, T.A. (1993). Masks made easy. *CCP4/ESF-EACBM Newsletter on Protein Crystallography*. **28**, 56–59.

47. Jones, T.A. (1992). *A, yaap, asap, @#*? a set of averaging programs.* In *Molecular Replacement.* (Dobson, E.J., Gover, S. & Wolf, W., eds), pp. 91–105, SERC Daresbury Laboratory, Warrington, UK.

48. Brünger, A.T. (1992). *X-PLOR Version 3.1: a System for X-ray Crystallography and NMR*. Yale University Press, New Haven, CT.

49. Collaborative Computational Project, No.4. (1994). The CCP4 suite: programs for protein crystallography. *Acta Cryst. D* **50**, 760–763.

50. Laskowski, R.A., MacArthur, M.W., Moss, D.S. & Thornton, J.M. (1993). Automated refinement of protein models. *Acta Cryst. D* **49**, 127–149.

51. Laskowski, R.A., MacArthur, M.W., Moss, D.S. & Thornton, J.M. (1993). PROCHECK: a program to check the stereochemical quality of protein structures. *J. Appl. Cryst.* **26**, 283–291.

52. Luzzati, V. (1952). Traitement statistique des erreurs dans la determination des structures cristallines. *Acta Cryst.* **5**, 802–810.

53. Read, R.J. (1986). Improved Fourier coefficients for maps using phases from partial structures with errors. *Acta Cryst. A* **42**, 140–149.

54. Jones, T.A., Zou, J.-Y., Cowan, S.W. & Kjeldgaard, M. (1991). Improved methods for building protein models in electron density maps and the location of errors in these models. *Acta Cryst. A* **47**, 110–119.

55. Richards, F.M. & Lee, B. (1971). The interpretation of protein structures: estimation of static accessibility. *J. Mol. Biol.* **55**, 379–400.

56. Kleywegt, G.J. & Jones, T.A. (1994). A super position. *CCP4/ESF-EACBM Newsletter on Protein Crystallography*. **31**, 9–14.

57. Kabsch, W. (1978). A discussion of the solution for the best rotation to relate two sets of vectors. *Acta Cryst. A* **34**, 827–828.

58. Kraulis, P.J. (1991). MOLSCRIPT: a program to produce both detailed and schematic plots of protein structures. *J. Appl. Cryst.* **24**, 946–950.

59. Carson, M. (1987). Ribbon models of macromolecules. *J. Mol. Graph.* **5**, 103–106.

60. Merritt, E.A. & Murphy, M.E.P. (1994). Raster3D version 2.0, a program for photorealistic molecular graphics. *Acta Cryst. D* **50**, 869–873.

61. Nicholls, A. & Honig, B. (1991). A rapid finite difference algorithm, utilizing successive over-relaxation to solve the Poisson–Boltzmann equation. *J. Comput. Chem.* **12**, 435–445.